

EXPLORATORY DYNAMIC MATERIAL CHARACTERIZING TESTS ON ULTRA-HIGH PERFORMANCE FIBRE REINFORCED CONCRETE

J Isaacs, University of California at San Diego, USA
J Magallanes*, Karagozian & Case, USA
M Rebentrost, VSL Australia, Australia
G Wight, VSL Australia, Australia

Abstract

This paper describes the results of exploratory dynamic material characterization tests performed on an ultra-high performance fiber reinforced concrete (UHPFRC) of the reactive powder concrete (RPC) type known under the brand name of Ductal®. The tests were conducted with a split Hopkinson pressure bar (SPHB) using novel techniques developed by the University of California at San Diego Center of Excellence for Advanced Materials (UCSD-CEAM). Compression and tension tests on unconfined UHPFRC specimens were conducted to examine the behavior of the material to various loading rates and initial damage states. The results indicate that the compression strength of Ductal® increases with increasing loading rate, as has been measured for other cementitious materials. In addition, the material exhibits significant levels of residual strength and stiffness after being damaged by initial compression loads. In tension, the material exhibits post peak tension softening with residual strengths over one third of its peak strength.

Keywords: loading rate effects, split Hopkinson pressure bar, ultra high performance steel reinforced concrete, reactive powder concrete

1. Introduction

RPC is a cementitious material consisting of cement, sand, silica fume, silica flour, superplastizer, water and high strength steel fibers. The present material, marketed under the brand name of Ductal®, was first described in the literature in [1] and further developed by Bouygues, the parent company of VSL, Lafarge and Rhodia.

The use of UHPFRC has become more widespread in structural applications in recent years. RPC is almost self-placing, has compressive strengths over 150 MPa and flexural strengths of 25 to 30 MPa [2, 3]. UHPFRC has also been shown to exhibit extraordinary durability properties in comparison to ordinary concretes [4]. While engineering structures constructed from UHPFRC are not intended to replace ordinary reinforced concrete applications, the use of UHPFRC around the world has increased in recent years particularly for pedestrian and road bridges [5, 6], architectural applications [7, 8] and other structural engineering applications that exploit the mechanical and durability properties. Design guidelines for UHPFRC limit analysis are now widely available [9, 10].

Most recently, laboratory and experimental field tests have demonstrated that the material exhibits enhanced resilience against shock and impact loads. Reinforced UHPFRC panels subjected to large explosive loads displayed high levels of ductility and no signs of fragmentation [11]. A series of similar field tests using smaller near-contact high explosives showed resilience of UHPFRC to scabbing and spalling, even after repeated exposure to the same explosive [12]. Recent ballistic tests

showed that 100 mm thick UHPFRC panels passed certification for NATO standard 7.62/9.3 g full metal case bullets at 850 m/s (R2 rating), armour piercing 7.62 mm bullets, and two types of fragment simulating projectiles (FSP): a 50 caliber (13 mm diameter) and 20 mm diameter FSP. Comparisons with conventional panels indicate 125 mm of reinforced concrete or 190 mm of concrete block masonry is required to stop 7.62 full metal case bullets without perforation [13].

While these trials point to the efficacy of UHPFRC to blast and impact-resilient infrastructure, little definitive material response data is available that is needed by the engineering communities to properly develop and deploy designs for such applications. Carefully executed material response data, under both quasi-static and dynamic loads, are needed to properly develop simplified engineering models and to develop constitutive models for more advanced physics-based finite element models.

In this present study, we describe a set of exploratory dynamic material characterization tests performed on the Ductal® UHPFRC. The tests are executed with the split Hopkinson pressure bar (SHPB) using novel experimental techniques developed by the University of California at San Diego Center of Excellence for Advanced Materials (UCSD-CEAM). Compression and tension tests on unconfined UHPFRC specimens were conducted to explore the behavior of the material to various loading rates and initial damage states. The results indicate that Ductal® exhibits increases in compression strength with increasing loading rate. In addition, the material exhibits significant levels of residual strength and stiffness after being damaged by initial compression loads. In tension, the material exhibits post peak tension softening with residual strengths over one third of its peak strength.

2. Research Significance

Available data indicates that UHPFRC exhibits behaviors common to many cementitious materials including concrete. Quasi-static data shows that the material exhibits confinement effects, ductile or brittle deformations depending on the level of confinement, dilatancy due to shear, and volumetric compaction [14]. Each of these material behaviors is important to quantify to properly design structures constructed with UHPFRC.

Although rate effects have been noted for UHPFRC/RPC, a consistent set of data is not available. Several investigators have measured increases in compressive strength at elevated loading rates, but have concluded that the material exhibits less rate sensitivity than normal strength concrete (NSC) [15-17]. Based on our review of the literature, no reliable data exists for rate effects behaviors in tension. Despite a few studies regarding UHPFRC subjected to quasi-static direct tension [18, 19] or indirect tension [20-22], little is known on the tension/extension properties of the material.

Our present study offers important material response data under simple and measurable compression and tension loading paths that is needed to study the behavior of the material. Novel experimental techniques are used that show marked potential to further characterize UHPFRC.

3. Experimental Program

3.1 Principles

The SHPB, often referred to as the Kolsky bar [23], is a device that allows not only the loading of a specimen at strain rates ranging from under 100 s^{-1} to more than $10,000\text{ s}^{-1}$, but it is also a device capable of measuring the strain, strain rate and stress of the sample, each as a function of time. A specimen is placed in series between two long elastic bars, called the incident and the transmission bars, and a dynamic loading device, usually a gas gun with an elastic striker bar, imparts a uniaxial stress pulse to the incident bar. All three bars (the incident, transmission, and striker bars) are made of the same high strength material. If this impact is sufficiently intense, the sample will be loaded to failure.

The induced elastic stress pulse travels in the incident bar at the bars sound velocity and reaches the specimen after a finite time increment. When it does, and because the specimen is not acoustically impedance-matched with the bar, some of the wave energy will be transmitted through the specimen to the transmitter bar and the rest will be reflected back into the incident bar, while the specimen is deforming. In this sense the SHPB is a device which allows one to load specimens in very short time spans, from tens of microseconds to hundreds of microseconds. From the history of the transmitted pulse, one calculates the stress in the sample, using the strain record obtained through a strain gauge placed appropriately on the transmission bar, and from the time-history of the reflected pulse, one estimates the strain in the sample (actually the time-history of the change in the sample length) by integrating the strain measured by the strain gauge suitably attached to the incident

bar.

The mechanics of one-dimensional uniaxial stress waves in solids provide the equations needed to deduce the load and deformations in the specimen from the data recorded from the strain gauges [24]. The most relevant equations for the purposes of describing these experiments are:

$$\dot{\varepsilon}_a(t) = \frac{2 \cdot C_0 \cdot \varepsilon_r(t)}{L_s} \quad (\text{Eq. 1})$$

$$\varepsilon_a(t) = \int_0^t \dot{\varepsilon}_a(t) dt \quad (\text{Eq. 2})$$

$$\sigma_a(t) = \frac{A_b}{A_s} \cdot E_b \cdot \varepsilon_a(t) \quad (\text{Eq. 3})$$

where, $\varepsilon_r(t)$ and $\varepsilon_a(t)$ are the reflected and transmitted strain histories, respectively; A_b , E_b , and C_0 are the bar's area, Modulus of Elasticity, and sound speed; A_s and L_s are the sample area and length, and $\varepsilon_a(t)$, $\dot{\varepsilon}_a(t)$, and $\sigma_a(t)$ are the reduced sample strain, strain rate, and stress histories as a function of time, t .

It should be noted that Eq. 1-3 are based on conservation of momentum, essentially that the length of the sample can be ignored; this is termed "equilibrium". It is also relevant to point out that second-order effects require consideration for both the test and specimen design and the reduction procedures of the raw data. Thorough discussions of the theory, design, data reduction procedures, and limitation of the SHPB are widely available in the literature and are not reiterated here for the sake of brevity.

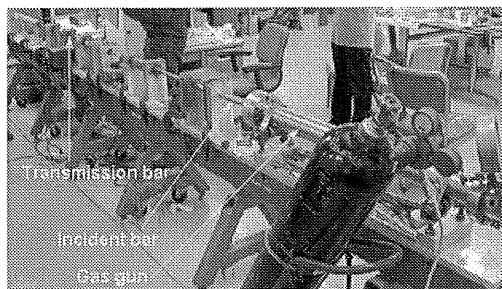
3.2 Test Setup

The SHPB tests were carried out at the UCSD-CEAM laboratories. The compression tests were conducted using a 19 mm diameter SHPB, while the tension tests were conducted using a 76.2 mm diameter SHPB.

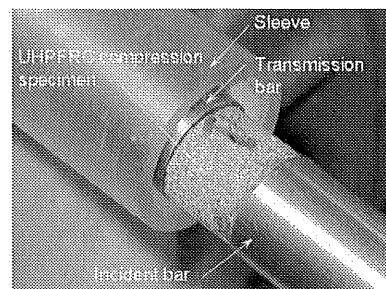
For the compression tests, a pair of 19 mm diameter, 1.2 m long Maraging Steel bars were used for both the incident and transmitter bars (Fig. 1). A gas gun with a 1.6 m barrel was used to propel the striker bar. Sample sizes were 18 mm diameter cylinders with a length of 15mm.

For the tension tests, a novel test design was developed by UCSD-CEAM using a pair of 76.2 mm diameter, 2.44 m long 7075 Aluminum bars for both the incident and transmitter bars. To produce the direct tension pulse, a push-pull arrangement was developed and utilized, as shown in Fig. 2. A two piece stepped flange was fabricated for the incident bar as well as a variety of striker tubes. A gas gun with a piston and crosshead were connected to the striker tube with aluminum rods. Firing the gas gun pushed the piston down the barrel, all the while pushing on the cross head, which in turn pulled the striker tube along the shaft of the incident bar. The striker tube then contacted the incident flange generating the desired tension pulse.

This scheme employed 76.2 mm tension samples that were adhered to the incident and transmitter bars using a commercially available epoxy. A notch was used to force the failure to occur in the center of the sample rather than at the ends. This required a somewhat longer specimen with a length to diameter (l/d) ratio approximately equal to two. The notch was designed as 57.2 mm in diameter, a reduction in area of 44% over the ends, sufficient to avoid fracture at the glue line.

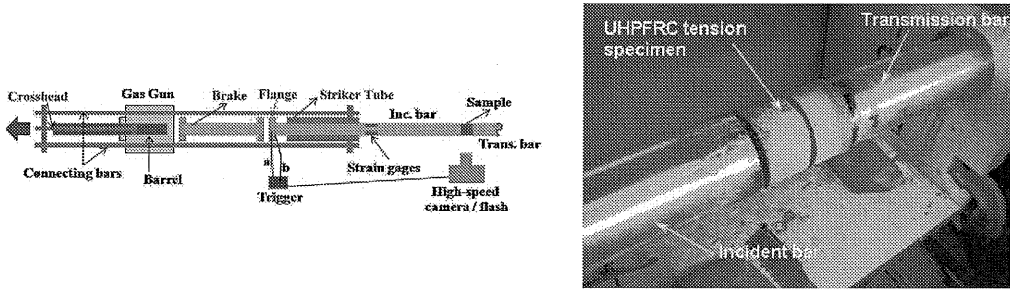


(a) 19 mm SHPB.



(b) Compression sample.

Fig. 1. Test setup for compression tests.



(a) Schematic of the UCSD-CEAM direct tension test.

(b) Tension sample.

Fig. 2. Test setup for tension tests.

3.3 Load Pulse Design

For analytical and modeling purposes it is desirable that SHPB tests be conducted at a constant strain rate, which is difficult to achieve for brittle materials [25, 26]. Load pulses were designed by controlling the amplitude and rise time of the pulse using various striker bars, impact velocities, and with the use of pulse shaping techniques [25]. For this series of tests, target strain rates chosen were as follows: the highest possible strain rate, the lowest possible strain rate as well as a representative strain rate between the two.

In the case of the compression test, the highest possible strain rate was determined by the equilibrium condition, i.e., the sample must be in equilibrium or near equilibrium at failure, this was determined from the experimental data. In the case of the tension test, the highest possible strain rate was determined by the actual strength of the material in tension, which was ultimately governed by the incident bar-sample bond.

For both compression and tension, the lowest possible strain rate required several considerations. Obviously, the loading pulse is required to be of sufficient amplitude to deform and eventually fail the sample. To achieve a low strain rate, the difference between the incident driving pulse and the transmitted pulse must be small because this is what effectively determines the strain rate. It was also necessary to shape the pulse so the rise time is as long as possible.

4. Test Results

4.1 Compression Tests

The UHPFRC specimens clearly exhibited increasing strength with increasing loading rates. This is shown in Fig. 3. Stress versus strain data is shown in Fig. 3a for three samples tested to failure using three different load pulses. The strain rate at peak strength is reported on each curve, which indicate peak strengths of 250 MPa (Test 12), 291 MPa (Test 5), and 312 MPa (Test 4) for strain rates of 185 s^{-1} , 471 s^{-1} , and $1,180 \text{ s}^{-1}$, respectively.

Comparisons of this data with data available in the literature show similar increases in strength. Peak strength versus strain rate data for ten of our tests are plotted in Fig. 3b, along with data obtained by other researchers on similar UHPFRC samples. As a baseline, the CEB Model [27] for concrete compressive strength as a function of strain rate is shown on the plot for a 40 MPa NSC. Several observations can be made from these comparisons. First, it is clear that our results are consistent with the other UHPFRC data. Second, Ductal® exhibits higher strengths than the other UHPFRC data at the same strain rate; we were also able to obtain data at much higher strain rates than obtained in the previous studies. Finally, it appears based on these exploratory results and the modified CEB Model, that UHPFRC exhibits similar increases in strength to NSC for strain rates in the range of 100 to $1,000 \text{ s}^{-1}$.

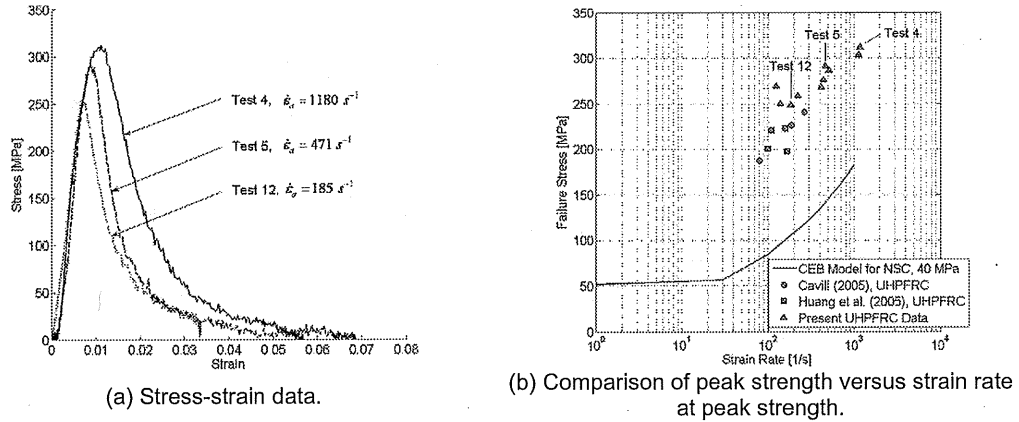
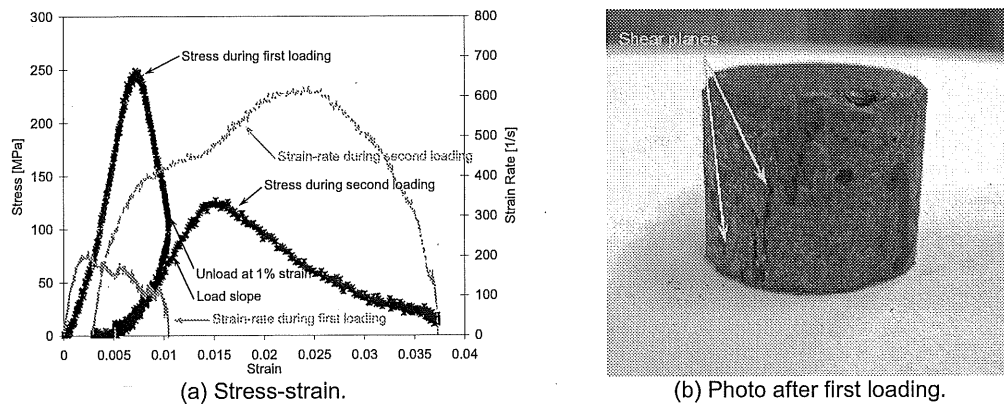


Fig. 3. Results of compression tests.

Several exploratory tests, employing dynamic recovery techniques developed at UCSD-CEAM [25], reveal that unconfined UHPFRC samples retain their load-carrying capacity when partially damage by an initial loading pulse. With reference to the results shown for Test 12 in Fig. 3a, Fig. 4a shows the results of a sample loaded with an identical loading pulse as Test 12, except the pulse was truncated by using a shorter striker bar (at the same velocity) and the specimen was recovered without further damage using dynamic recovery/moment trapping. This effectively unloaded the sample at a strain of approximately 1%. A posttest photo of the sample is shown in Fig. 4b and displays the typical failure patterns observed in all compression tests, where diagonal shear planes develop that remain bridged by the steel reinforcing fibers. Another load pulse was next applied to this damaged specimen and deformed until failure. The stress versus strain results are shown in Fig. 4a and posttest photographs of the failed specimens are presented in Fig. 4c and 4d. The photos evidence that additional shear planes developed during this second loading, which eventually fragmented the sample into several pieces. Several of the larger pieces remained connected by the steel fibers.

The stress-strain data shown in Fig. 4a demonstrate that UHPFRC retains significant levels of residual strength and stiffness when loaded beyond its peak strength. Note that the initial slope of the stress-strain curve (i.e., the Modulus of Elasticity or modulus) during the second loading is less than the modulus of the undamaged specimen; this behavior is indicative of the internal damage incurred during the first loading. Also note that the unload modulus during the first loading is very similar to the loading modulus during the second loading; this is evidence of residual stiffness. The peak strength during the second loading was 128 MPa, over half of the strength of an undamaged specimen. This is a remarkable capability for a cementitious material, especially when considering that NSC achieves peak unconfined strengths at strains between 0.2 to 0.3% with little or no residual strength or stiffness when loaded beyond the peak strain.



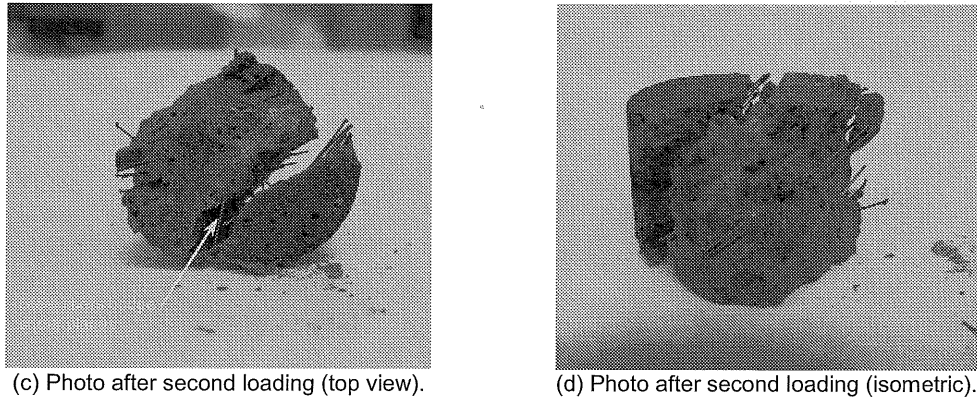


Fig. 4. Behavior of material in compression with initial damage.

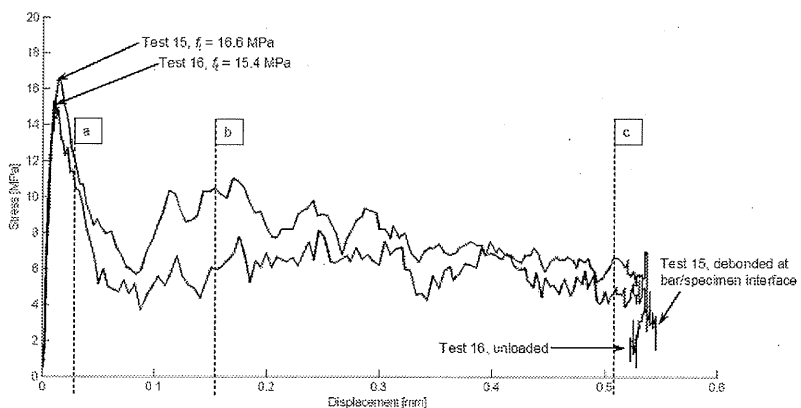


Fig. 5. Results of initial tension tests in stress versus displacement.

4.2 Tension Tests

For direct tension tests, it is common to study the response of cementitious materials in stress versus displacement quantities, the latter of which is sometimes referred to as the crack opening displacement (COD). Integration of a stress versus COD curve yields the material fracture energy, G_f , which is a commonly reported property of these types of materials.

Stress versus displacement curves from Test 15 and 16 are shown in Fig. 5, which were subjected to average strain rates roughly 100 s^{-1} . Peak strengths for these two tests were measured as 16.6 and 15.4 MPa, respectively, and the displacement at peak strength was 0.0147 mm and 0.0114 mm, respectively. Similar to concrete, the strength quickly decays after reaching its peak strength; however, unique to the present material, residual tension strengths are observed. The residual strength range from 6 to 10 MPa, initiating at a displacement close to 0.1 mm, and slowly decay with further deformation. Test 15 was unloaded at a displacement slightly over 0.5 mm, while the sample/bar interface for Test 16 failed at approximately the same level of displacement. This data yields fracture energies, G_f , of 4,310 and 3,350 N·m/m² for Test 15 and 16, respectively. Typical NSC concretes exhibit G_f quantities ranging from 50 to 300 N·m/m² under quasi-static loads [27].

Most of this deformation capacity appears to be facilitated by the steel reinforcing fibers. Cracks in the samples are highly localized and appear to traverse around voids and/or internal defects. Crack opening is retarded by the steel reinforcing fibers perpendicular to the crack. Fig. 6 shows high speed photographs near the surface of the notch for Test 16 at several displacements depicted in Fig. 5; these are denoted (a) at a displacement shortly after the peak strength, (b) at a displacement of approximately 0.15 mm, and (c) at a displacement slightly over 0.5 mm. Various small cracks become visible at a displacement of 0.15 mm, while at 0.5 mm, the cracks have clearly grown both normal and parallel to the direction of the applied tension loading. Posttest inspection indicated the sample had not formed a complete fracture plane and the sample could have sustained additional displacement

prior to failure.

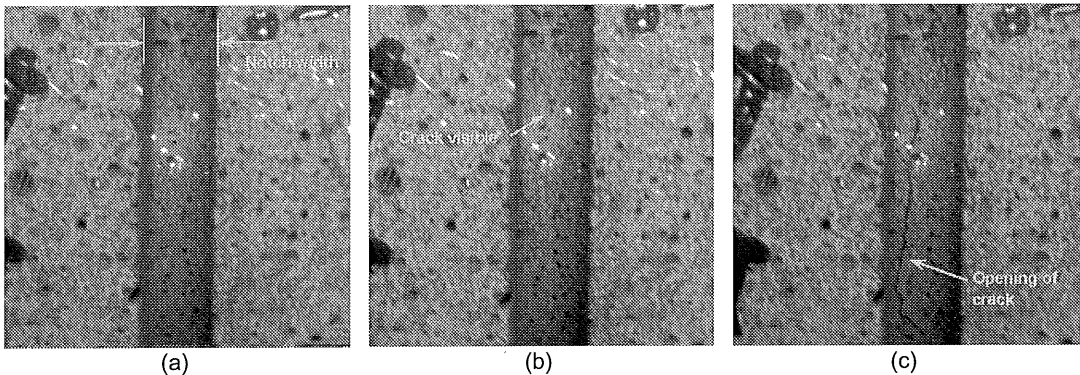


Fig. 6. High speed photographs of crack propagation (refer to Fig. 5).

5. Conclusions

This paper described a set of results from exploratory dynamic material tests aimed at characterizing a UHPFRC/RPC material known under the brand name of Ductal®. The tests employed the split-Hopkinson pressure bar, using novel experimental techniques, to induce dynamic compression and tension loads in unconfined UHPFRC samples. The compression results indicate that the materials strength increases as a function of loading rate, similar to that observed in concrete and other cementitious materials. In addition, the material exhibits significant levels of strength and stiffness after being loaded in compression beyond its peak strength. In tension, the material exhibits a post peak softening branch commonly observed in normal strength concrete, but retains over one third of its peak strength in residual tension strength. As a result, the material exhibited tensile fracture energies at least an order of magnitude greater than is typical of normal strength concrete under quasi-static loads.

More research is needed to complete characterization of UHPFRC, especially in tension, where the effect of loading rate on the strength, failure mode and energy absorption characteristics of the material remain unquantified. The Hopkinson bar techniques developed and deployed for this exploratory effort are shown to have significant potential to further characterize this phenomenon.

6. Acknowledgements

The authors acknowledge VSL Australia for their direct support of the testing program and supply of Ductal® test specimen. Also, the technical review and editing of this paper by Mr. John Crawford of Karagozian & Case was greatly appreciated.

7. References

- [1] RICHARD P., and CHEYREZY M., "Composition of Reactive Powder Concrete", *Cement and Concrete Research*, Vol. 25, No. 7, 1995, pp.1501-1511.
- [2] GOWRIPALAN N., WATTERS R., GILBERT I., and CAVILL B., "Reactive Powder Concrete for Precast Structural Concrete – Research and Development in Australia", *Proc. 21st Biennial Conference of the Concrete Institute of Australia*, Brisbane, Australia, 2003.
- [3] ACKER P., and BEHLOUL M., "Ductal Technology: A Large Spectrum of Properties, A Wide Range of Applications", *Proc. of the fib Symposium*, Avignon, France, 2004.
- [4] ROUX N., ANDRADE C., and SANJUAN M.A., "Experimental Study of Durability of Reactive Powder Concretes", *Journal of Materials in Civil Engineering*, Vol. 8, No. 1, 1996, pp. 1-6.
- [5] REBENTROST M., and CAVILL B., "Reactive Powder Concrete Bridges", *Proc. AustRoads 6th Bridge Conference*, Perth, Australia, 2006.
- [6] BLAIS P.Y., and COUTURE M., "Precast, Prestressed Pedestrian Bridge – World's First Reactive Powder Concrete Structure", *PCI Journal*, Sept.-Oct. 1999, pp. 61-71.
- [7] RICCIOTTI, "Bridge to the Future", *ASCE Civil Engineering Magazine*, Vol 71 No 1, November 2001.
- [8] VINCENZINO E., CULHAM G., PERRY V., ZAKARIASEN D., and CHOW T., "First Use of UHPFRC in Thin Precast Concrete Roof Shell for Canadian LRT Station", *PCI Journal*, USA, September-October, 2005, pp 50-67.

- [9] GOWRIPALAN N., and GILBERT R.I., "Design Guidelines for Ductal Prestressed Concrete Beams. Design Guide", Civil & Environmental Engineering School, University of NSW, Sydney, Australia, 2000.
- [10] AFGC / SETRA WORKING GROUP, "Ultra High Performance Fibre-Reinforced Concrete – Interim Recommendations", Report, Association Française de Génie Civil, Paris, France, 2002.
- [11] NGO T., MENDIS P., LAM N. and CAVILL B. "Performance of Ultra-High Strength Concrete Panels subjected to Blast Loading", *The 2005 Science, Engineering and Technology Summit*, Canberra, July 2005.
- [12] KUZNETSOV V., REBENTROST M., and WASCH J., "Strength and Toughness of Steel Fibre Reinforced Reactive Powder Concrete Under Blast Loading", *1st International Conference on Analysis and Design of Structures Against Explosive and Impact Loads*, Tianjin, China, Sept. 2006.
- [13] GUPTA A., MENDIS P., NGO T. and REBENTROST M., "Modelling Localised Response of Steel Fibre Reinforced Ultra High-Strength Concrete Panels Under High Velocity Impact", *Australasian Conference of Materials and Structural Mechanics*, Christchurch, New Zealand, 2006.
- [14] WILLIAMS, E.M., GRAHAM, S.S., AKERS, S.A., REED, P.A., and T.S. RUSHING, "Mechanical properties of baseline UHPC with and without steel fibers," *Computational Methods and Experiments in Material Characterisation IV*, Eds. A.A. Mammoli and C.A. Brebbia, WIT Press, Southampton, 2009.
- [15] LOK, T.S., ZHAO, P.J., and G. LU, "Using the split Hopkinson pressure bar to investigate the dynamic behavior of SFRC," *Magazine of Concrete Research*, Vol. 23, No. 2, pp.183-191, April, 2003.
- [16] CAVILL, B., "An ultra-high performance material for resistance to blasts and impacts," *Proc. 6th Asia-Pacific Conference on Shock and Impact Loads on Structures*, Perth, Australia, Dec. 7-9, 2005.
- [17] HUANG, Z.Y., WANG, Y., XIAO, Y., and F.Y. LU, "Dynamic behavior of reactive powder concrete in split Hopkinson pressure bar testing," *Proc. 6th Asia-Pacific Conference on Shock and Impact Loads on Structures*, Perth, Australia, Dec. 7-9, 2005.
- [18] BARRAGÁN, B.E., GETTU, R., MARTÍN, M.A., and R.L. ZERBINO, "Uniaxial tension test for steel fibre reinforced concrete – a parameteric study," *Cement & Concrete Composites*, Vol. 25, No. 7, October, 2003, pp. 767-777.
- [19] MALEEJ, M., QUEK, S.T., and J. ZHANG, "Behavior of Hybrid-Fiber Engineering Cementitious Composites Subjected to Dynamic Tensile Loading and Projectile Impact," *ASCE Journal of Materials in Civil Engineering*, Vol. 17, No. 2, March/April, 2005, pp. 143-152.
- [20] TAYLOR, M., LYDON, F.D., and B.I.G. BARR, "Toughness Measurements on Steel Fibre-reinforced High Strength Concrete," *Cement & Concrete Composites*, Vol. 19, No. 4, 1997, pp. 329-340.
- [21] LEE, M.K., and B.I.G. BARR, "Strength and fracture properties of industrially prepared steel fibre reinforced concrete," *Cement & Concrete Composites*, Vol. 25, No. 3, 2003, pp. 321-332.
- [22] SIVAKUMAR, A., and M. SANTHANAM, "Mechanical properties of high strength concrete reinforced with metallic and non-metallic fibres," *Cement & Concrete Composites*, Vol. 29, No. 8, 2007, pp. 603-608.
- [23] KOLSKY, H., "An Investigation of the Mechanical Properties of Materials at Very High Rates of Loading," *Proceedings of the Royal Society of London*, B.62, pp. 676-700, 1949.
- [24] GRAY, G.T., "Classic Split-Hopkinson Pressure Bar Technique: Chapter 6A," Los Alamos National Laboratory Technical Report, LA-UR-99-2347, May 1999.
- [25] NEMAT-NASSER, S., J.B. ISSACS, and J.E. STARRETT, "Hopkinson techniques for dynamic recover experiments," *Mathematical and Physical Sciences*, Vol. 435, Issue 1894, Nov., 1991, pp. 371-391.
- [26] FREW, D.J., FORRESTAL, M.J., and W. CHEN, "Pulse Shaping Techniques for Testing Brittle Materials with a Split Hopkinson Pressure Bar," *Experimental Mechanics*, Vol. 42, No. 1, March, 2002, pp. 93-106.
- [27] COMITÉ EUROPÉEN INTERNATIONAL DU BÉTON (CEB), *CEB-FIP Model Code 1990*, Redwood Books, Trowbridge, Wiltshire, U.K.